Semi-automated segmentation of the entire left ventricle from 3D cine DENSE MRI using Guide-Point Modeling

Daniel Alejandro Auger[1], Xiaodong Zhong[2], Frederick H Epstein[3], Ernesta M Meintjes[1], and Bruce S Spottiswoode[4]

[1]MRC/UCT Medical Imaging Research Unit, Department of Human Biology, University of Cape Town, Cape Town, Western Cape, South Africa, [2]MR R&D Collaborations, Siemens Medical Solutions, Atlanta, Georgia, United States, [3]Departments of Radiology and Biomedical Engineering, University of Virginia, Charlottesville, Virginia, United States, [4]Cardiovascular MR R&D, Siemens Medical Solutions, Chicago, Illinois, United States

Target Audience: Researchers and clinicians assessing myocardial strain, and any individual interested in geometric models of the heart, post-processing, and image segmentation with 3D MRI data.

Purpose: Regional mechanical strain has been shown to be a useful clinical indicator of myocardial function. DENSE is a quantitative cardiac wall imaging technique, which encodes tissue displacement directly into the phase of the stimulated echo (typically with reference to end diastole) [1]. A free-breathing navigator-gated 3D spiral cine DENSE sequence has been developed to quantify tissue motion and strain within the entire left ventricle (LV) in a single scan [2]. An essential step during the post-imaging data analysis is defining the epicardial and endocardial boundaries of the LV. A 3D cine DENSE data set typically requires over 600 epicardial and endocardial LV contours, which would take an experienced user over an hour to demarcate. The adoption of this technique is therefore limited by this necessary but prohibitively time consuming step. The purpose of this study was to implement a semi-automated LV segmentation algorithm for 3D cine DENSE MRI.

Methods: In accordance with protocols approved by the University of Virginia Institutional Review Board, whole heart data were acquired from 4 healthy volunteers on a 1.5T Siemens Magnetom Avanto MRI scanner using a 3D spiral cine DENSE sequence [2]. The imaging volume was aligned along the long axis, and the spatial and temporal resolution was $2.8 \times 2.8 \times 5$ mm^3 and 32 ms, respectively. Imaging parameters included: ramped flip angle up to 20°, TR = 16 ms, TE = 1.3 ms, number of spiral interleaves = 6 and cardiac phases = 22. Fourteen 3D partitions were acquired, and zero-padding to 28 partitions was performed during reconstruction. The resulting 3D image matrix size was $128 \times 128 \times 22$. Three dimensional spatio-temporal phase unwrapping was performed to remove aliasing, and displacements were calculated for each voxel at each time point in the cardiac cycle. Eight epicardial and eight endocardial guide points per slice were interactively placed by a user on the cine DENSE magnitude images at any single time point (t_n), as shown in Figure 1. A 3D prolate-spheroidal LV geometrical model was fitted to the guide point positions, creating complete epicardial and endocardial surfaces [3]. As each DENSE displacement vector corresponds to the tissue position at the time of encoding, the initial guide points can be placed at any cardiac phase. Using 3D tissue tracking [4], each of the defined guide points was projected onto all other cardiac phases. The model was then re-fitted at each cardiac phase to correct for any errors which may have been introduced during tissue tracking. Spatial derivatives [5] and low SNR filtering steps were implemented as part of the 3D tissue tracking algorithm in order to remove the effects of image phase noise. A myocardial SNR threshold was introduced based on the signal enclosed in the first set of contours derived from the user defined guide points. The resulting trajectories were improved using temporal fitting with 10th order polynomials. Since the guide points are placed on the myocardial border, and the tissue tracking is only valid in the myocardium, an additional step was introduced to keep the guide points on the myocardial border. This involved representing each trajectory position at every frame by a 3D Gaussian function with an integrated intensity of unity. As the guide points are propagated across the cardiac cycle, their position is refined by moving each guide point along the intensity gradient of the combined Gaussian image towards the endocardial / epicardial boundary until a value of 0.5 is reached. All 4 data sets were manually contoured by a single operator, and three slices (apical, mid and basal) at a single time point were manually contoured by a second operator. Using the semi-automated contours and full set of manual contours, the LV volume was calculated at end diastole and end systole, and LV mass was calculated during end-diastole. A few short axis slices were typically excluded due to the inability to distinguish the LV, and volume estimates for these slices were extrapolated based on the adjacent slice. Further evaluation was done by comparing Dice and Jaccard coefficients [6], which represent the reproducibility and accuracy based on the spatial overlap of the manual and semi-automated contours. False positive and false negative mean area errors were further calculated. All software development was performed in MATLAB (Mathworks, Natick, MA).

Results: The complete semi-automated segmentation process took approximately 6-12 minutes per subject (4 min for guide point positioning and 8 min for computation). Example epicardial and endocardial surfaces during diastole and systole are shown in Figures 2 (a) and (b), respectively. The segmentation errors for a single mid ventricular slice, for all 4 data sets, based on the false positive and false negative mean area measurements are: 12.2±5.5% for Operator 1 vs 2; 12.8±3.1% for Operator 1 vs the algorithm, and 10.8±4.1% for Operator 2 vs the algorithm. The Jaccard and Dice similarity coefficients are: 0.8±0.04 and 0.9±0.02 for Operator 1 vs 2; 0.8±0.05 and 0.9±0.03 for Operator 1 vs the algorithm, and 0.8±0.04 and 0.9±0.02 for Operator 2 vs the algorithm, respectively. The volume and mass results are given in Table 1. As the entire LV was not included, LV function results are not comparable to previous LV studies. Figure 3 illustrates an example of the comparison between hand defined contours (a-c) and model defined contours (d-f).

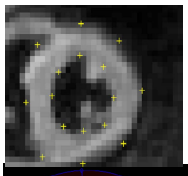

Figure 1: DENSE magnitude image with user defined guide points at the epicardial and endocardial borders.

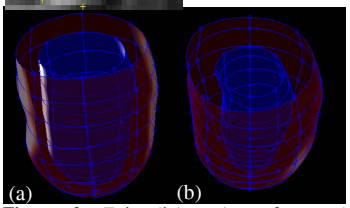

Figure 2: Epicardial (red) surface and endocardial (blue) surface at (a) end–diastole, (b) end-systole.

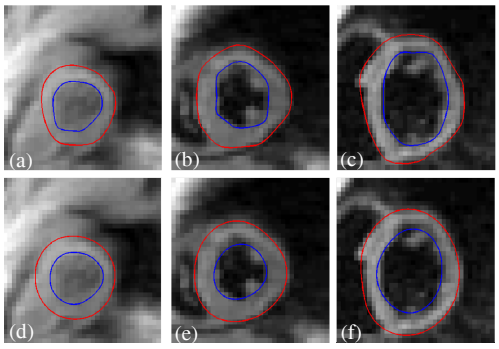

Figure 3: DENSE magnitude images, (a-c) manual defined epicardial (red) and endocardial (blue) contours, (d-f) model defined epicardial and endocardial contours. (a,d) Apical slice during end-diastole, (b,e) mid-ventricular slice during systole, and (c,f) basal slice during early-diastole.

Table 1: Comparing LV parameters. Mean ± 1SD.

Contour Method	EDS (ml)	ESV (ml)	SV (ml)	EF (%)	Mass (g)
Operator	164 ±17.27	77.66 ±6.34	85.09 ±13.22	51.69 ±2.58	163.88 ±9.56
Model	147.54 ±23.53	74.13 ±11.92	73.41 ±12.38	49.75 ±2.17	177.5 ±20.2
P(>0.05)	0.30	0.62	0.24	0.29	0.29

Discussion: There were no significant differences between manual and model volumes and mass, shown in Table 1. The agreement between inter-observer and algorithm vs manual variability demonstrates the accuracy of the algorithm. Out of a total of 2 124 contours, over all 4 data sets, only 125 (5.6%) of the semi-automated contours would need to be readjusted to better fit the LV myocardium. The error found using the Dice and Jaccard coefficients, which can be an indicator of precision, was less than 10 and 20% respectively, showing reasonable results. Computation time can be improved by implementing the algorithm in a language such as C++.

Conclusion: The guide point modeling approach to segmenting 3D cine DENSE data shows promising results, and offers at least a 10 fold reduction in the time taken to segment the LV myocardium. The LV parameter results compare favorably with previous studies, while similarity coefficients show the algorithms accuracy and reproducibility. This is a significant step towards the automation of the 3D cine DENSE data analysis.

References: 1. Aletras et al. Journal of Magnetic Resonance 137:247–252, 1999. **2.** Zhong et al. MRM, 64:1089-1097, 2010. **3.** Young et al. Radiology, 216:597-602, 2000. **4.** Auger et al. JCMR, 14: 4 2012. **5.** Spottiswoode et al. Medical Image Analysis,13:105-115, 2009. **6.** Zou et al. Acad Radiol, 11(2):178-189, 2004.